2A. 1 Bowing convective systems in a popular operational model: Are they for real?

Melissa S. Bukovsky*
University of Oklahoma, Norman, OK

John S. Kain and Michael E. Baldwin
University of Oklahoma/CIMMS/NSSL, Norman, OK

1. INTRODUCTION

Over the past several years, research scientists at the National Severe Storms Laboratory (NSSL) and Cooperative Institute for Mesoscale Meteorological Studies (CIMMS) have collaborated with forecasters at the Storm Prediction Center (SPC) on a number of research projects. A particularly active area of investigation has involved operational forecast models (e.g., Kain et al. 2003). Since these models play such an important role in the forecast preparation process at the SPC and elsewhere, there has been a compelling interest in trying to identify and understand beneficial and misleading characteristic behaviors in the models. For example, Baldwin et al. (2002) showed that unrealistic vertical structures are often apparent in model-output soundings from the Eta model (Black 1994; now called the NAM – North American Mesoscale model). Identification of these structures can help forecasters to make more informed assessments about the reliability of certain aspects of the model forecast (S. Weiss 2004, personal communication), enabling them to make better usage of the model guidance in preparing forecasts.

Over the years forecasters and researchers have also noticed that another characteristic feature sometimes emerges in forecasts from the Eta model, and more recently from the "beta" versions of the NMM (Nonhydrostatic Mesoscale Model – Janjic 2003). These two models use very similar physics packages, including the Betts-Miller-Janjic convective parameterization (Betts 1986; Janjic 1994; hereafter BMJ). The feature in question is characterized as a strongly bowing line segment. For example, Fig. 1 shows four instances of this phenomenon that were predicted by the Eta or NMM during the 2004 SPC/NSSL Spring Program (see Kain et al. 2005 for a description of this program). Fig. 1a shows a bow-shaped precipitation pattern over central Oklahoma. This spurious feature emerged several hours earlier from a localized area of convection over southeastern Kansas, taking shape on the southwestward periphery of a more circular area of convection. It gradually developed the characteristic elongated, bowing configuration as it moved towards the southwest in low-level south-southeasterly flow. Likewise, the bow in Fig. 1b grew out of a small area of convection near Milwaukee, rapidly expanding as it propagated to the south-southeast in predominantly southwesterly inflow. The two features in Figs 1c and d had similar origins but created even wider arcs, with the system in Fig. 1c nearly forming a complete circle of activity around the initial "blob" of convection.

Routine examination of output from the Eta and NMM reveals that these bow-shaped features occur with some regularity in these models, especially during the spring. Sometimes they appear in environments that support actual bow-echo development, but more often, as in each case highlighted by Fig. 1, they have no corresponding observational counterpart. They often have a shape and scale that is similar to typical bow echoes (see, e.g., Fujita 1955, Przybylinski 1995, and Weisman 2001 for an overview of bow echoes), at least in terms of their leading edge, but they rarely show any evidence of a "stratiform" rain region behind the bow-shaped line. Furthermore, very little, if any grid-scale precipitation is produced by the model with these systems. Nearly all of their precipitation is produced by the BMJ convective scheme.

So what are these features? How do they form and how do they move? What causes their characteristic shape? What value do they have to forecasters? The purpose of this study is to address these questions by examining an event in which prominent bow echoes were predicted by the Eta model and actually occurred, though with less than perfect correspondence to reality. We begin with a brief observational overview of the focal event, followed by a review of Eta model simulations, including an analysis of the fundamental characteristics of a primary bowing feature. This is followed by an assessment of the operative physical mechanisms involved in the upscale growth and propagation of this system, then a series of sensitivity tests that link the BMJ scheme to system behavior. We conclude with a discussion of the relevance of this work and the implications for forecasting propagating convective systems.

2. OBSERVATIONS

On the afternoon of 11 June 2001, a surface low-pressure system was positioned along the border of South Dakota and Minnesota (Fig. 2a). A warm front extended from this system eastward across south-central Minnesota, then curved southeastward nearly parallel to the Mississippi River in southwestern Wisconsin; a cold front extended to the south-southwest. A 15 – 20 m s^{-1} 850-hPa jet extending from the southern plains into Iowa and southern Minnesota

* *Corresponding author address:* Melissa S. Bukovsky, NSSL, 1313 Halley Circle, Norman, OK, 73069;
e-mail: melissa.bukovsky@noaa.gov

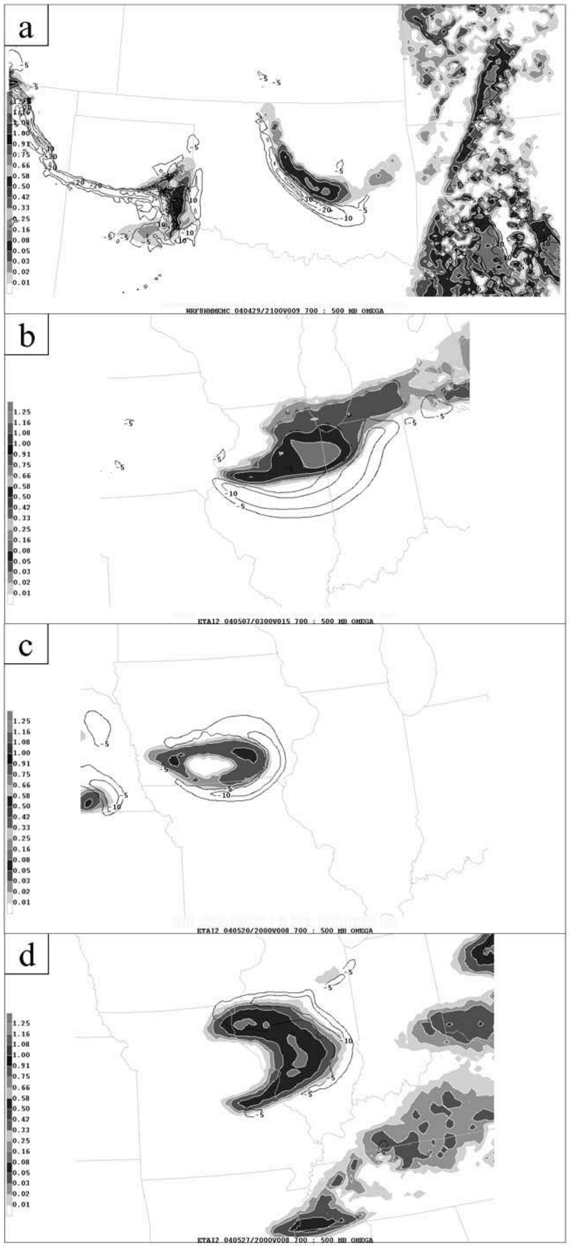

Fig. 2. 1h total precipitation accumulation (shaded) and mean 500-700 hPa pressure vertical velocity (contours at -5, -10, -20, -30, -40 dPa s^{-1}). a) 29 April 2004 2100 UTC forecast from the NMM. b) 7 May 2004 0300 UTC forecast from the operational Eta. c) 20 May 2004 2000 UTC forecast from the operational Eta. d) 27 May 2004 2000 UTC forecast from the operational Eta.

brought warm, moist air into this region (Fig. 2b), while strong mid and upper level winds prevailed across the northern states (Fig. 2c). A series of short-wave troughs was embedded in the flow, inducing areas of focused ascent. The environment was quite unstable and deep layer wind shear was also significant. For example, the 1800 UTC 11 June 2001 sounding from Chanhassen, MN (MPX) (location shown in Fig. 2a) revealed a mid-level (700-500 hPa) lapse rate of 8.6°C km^{-1}, a CAPE value of 3342 J kg^{-1} (most unstable parcel in the lowest 300mb), and a surface to 6-km shear value of 28 m s^{-1} (Fig. 3). The surface conditions farther south were warmer and moister, but also strongly capped, as 700-hPa temperatures hovered around 12°C in the warm sector (not shown). These conditions moved eastward with the surface low as time progressed.

Severe thunderstorms formed around 1800 UTC from west-central Minnesota into southeastern North Dakota. These storms evolved into a complex of supercellular, tornado producing storms along and just north of the warm front (Fig. 4). Storms also formed along the cold front but these storms were relatively weak and transient compared to the activity farther north.

As evening approached, the complex propagated southeastward into Wisconsin (Fig. 4). While entering the central portion of the state, around 0000 UTC 12 June 2001, the convective system began to display a quasi-linear mesoscale organization. Within a couple of hours, the system took on the form of a large bow echo and began producing a wide swath of wind damage. Propagation[1] took on an increasing southward component with time, and as the system neared Lake Michigan it showed evidence of a bookend vortex on the northeastern end of the line for several hours. Around 0600-0700 UTC on the 12th, after traversing much of Lake Michigan and parts of the bordering states and entering Indiana, the leading line began to weaken. Evidence of the complex still existed, though, into the daylight hours of that day.

3. ETA MODEL FORECAST

3.1 Model Configuration

The model configuration used to examine this June 2001 event is nearly identical to the operational Eta from this period (for a description of the Eta model, see Black 1994; Janjic 1994; and Zhao et al. 1997), with a few exceptions. First, integration occurs over a CONUS-sized subdomain rather than the entire Eta domain (Fig. 5). The smaller domain was used for experimental daily forecasts at the National Severe Storms Laboratory during 2001 (see Kain et al. 2003). The configuration includes 22-km grid spacing and 50 vertical layers, as in the 2001 operational code, but it uses fourth-order horizontal diffusion instead of the second order formulation used operationally. There is one other significant difference from the operational code. For diagnostic purposes, a change was made to call the BMJ convective parameterization every time step (instead of every sixth time step) so that quasi-continuous convective tendencies could be saved and examined. When this change was made, a related parameter was inadvertently left unchanged so that the relaxation time scale for convective adjustment was

[1] Use of the word 'propagation' herein refers to the component of the system motion that is not advective. It will not be used to reference the system movement as a whole.

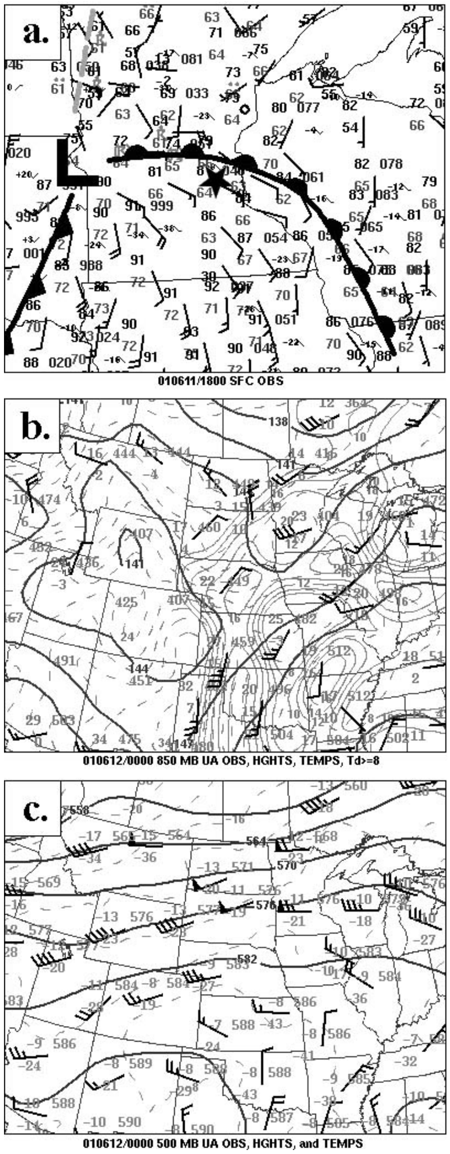

Fig. 2. Meteorological conditions on 11 June 2001. a) Surface analysis valid 1800 UTC, location of MPX indicated by star, b) 0000 UTC 12 June 2001 850 hPa observed winds, heights (dark grey lines, dam), temperatures (light grey, dashed lines, ºC), and dew point temperatures (light grey, solid lines, ºC), c) 0000 UTC 12 June 2001 500 hPa observed winds, heights (dark grey lines, dam), and temperatures (light grey dashed lines, ºC).

decreased by a factor of six. In other words, convective adjustment was prescribed to proceed six times faster than intended.

This oversight turned out to be serendipitous, as the modification resulted in a qualitatively similar, but more clearly defined and strongly propagating convective system with a more readily discernible relationship between convective forcing and mesoscale response. In effect, the signal-to-noise ratio increased with the faster convective adjustment, allowing us to more clearly diagnose the operative relationships between forcing and response amid the multitude of

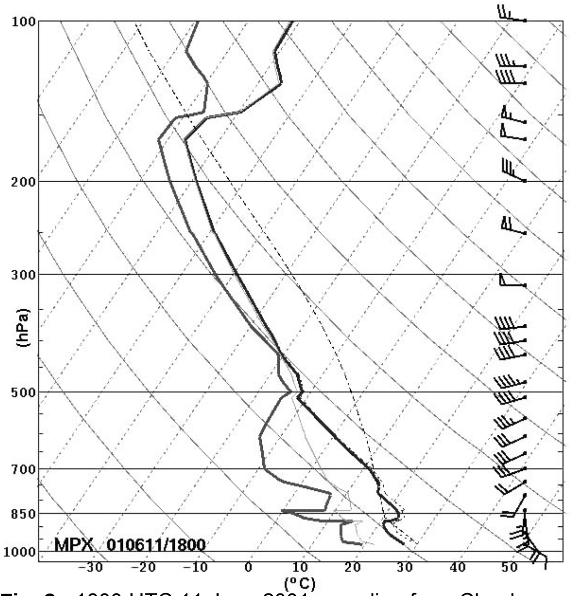

Fig. 3. 1800 UTC 11 June 2001 sounding from Chanhassen, MN (MPX).

structures and processes that permeate this real data simulation. Since our intent is to demonstrate these relationships as clearly as possible, the results shown herein focus on simulations using this modified convective feedback rate. A simulation produced using the operational convective adjustment settings is discussed briefly for comparison in section 4.

3.2 Overview of Simulation

The simulation begins at 0000 UTC 11 June 2001, using initial conditions from the operational Eta model. The model generates a bow-shaped, strongly propagating precipitation system, although the timing and location of the simulated system does not correspond particularly well with reality. The simulated system originates around 1000 UTC in the model as an isolated area of convection in northeastern South Dakota, upstream from the observed location in both time and space. By the 11 h time a weak meso-high has formed in this vicinity and a semi-circular convective outflow is developing (Fig. 6a and b). At 1500 UTC the radius of the outflow has expanded considerably and new development is focused on the southern and southeastern periphery as the system propagates to the southeast (Figs. 6c and d). This trend continues through the 18 h time as the system propagates into central Iowa (Figs. 6e and f). After this time, the system continues to expand, but it gradually weakens and dissipates (Fig. 7a). The configuration of the system and its direction of movement have obvious parallels with the observed convective complex. While this correspondence is intriguing, similar systems that have no observational counterpart develop in the model with some regularity. Thus, rather than judge this simulation as a success or failure for the model, we choose to focus on the dynamic mechanisms of system formation

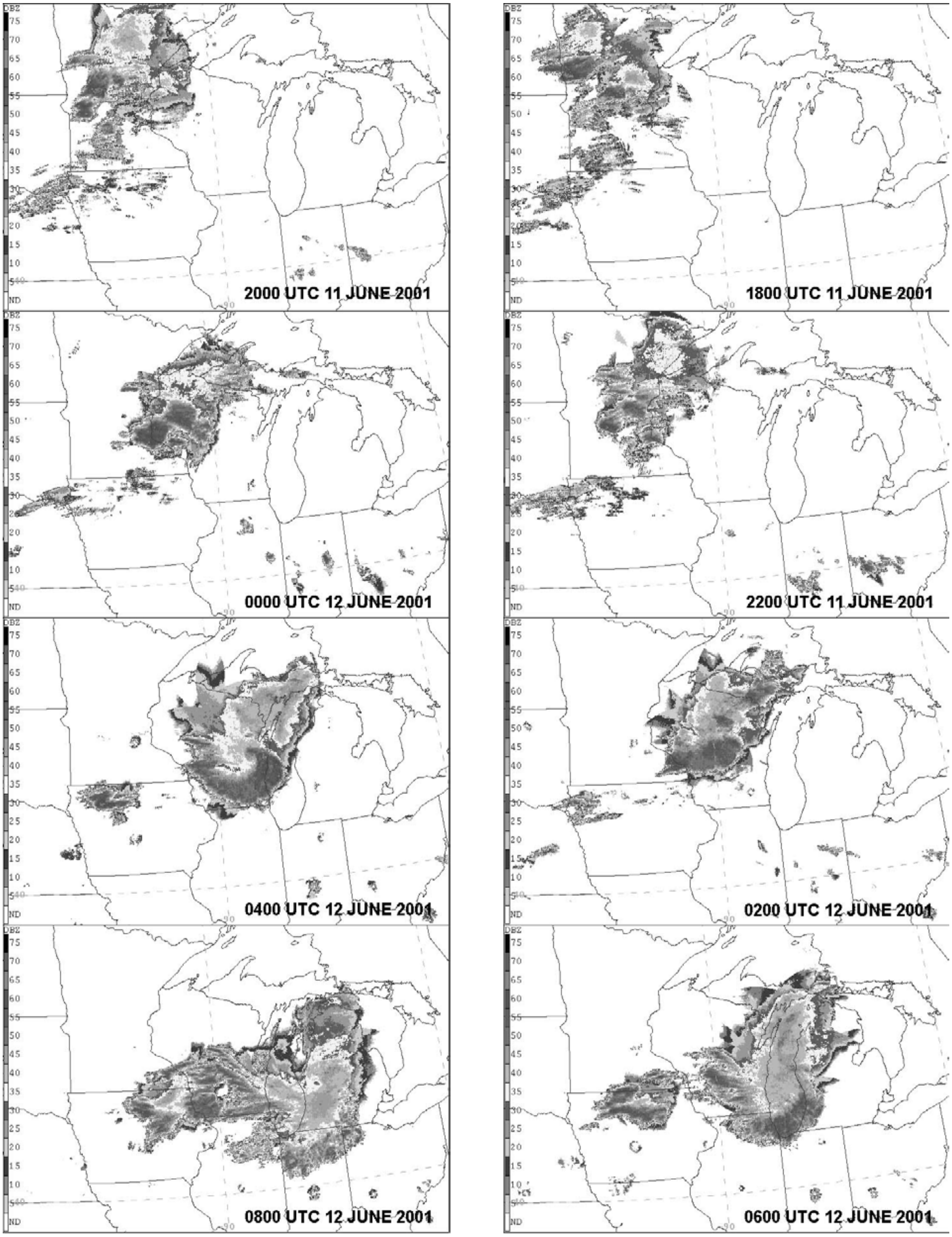

Fig. 4. 1 hourly composite base reflectivity displayed as the maximum reflectivity within the past hour at each pixel, shown every two hours from 1800 UTC 11 June 2001 to 0800 UTC 12 June 2001.

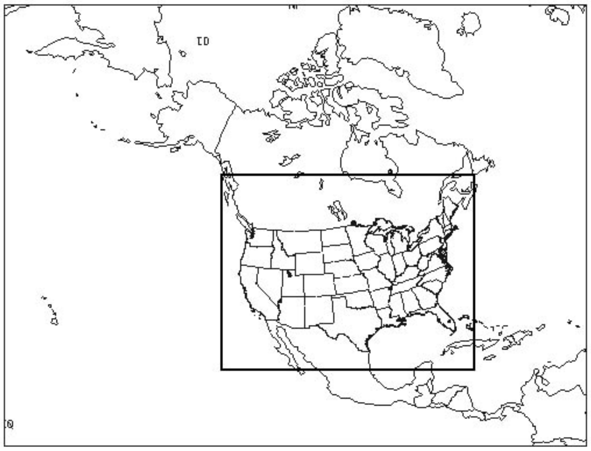

Fig. 5. Computational domain for all Eta model simulations (inset) shown within the full operational domain as of June 2001.

and propagation in the model. This simulation is hereafter referred to as the control run.

3.3 Diagnosing dynamic factors that promote propagating and bowing characteristics

Model output soundings are examined routinely by forecasters at the SPC and by research scientists working with these forecasters. Many such soundings have been examined in the vicinity of bowing, propagating convective systems that appear in Eta model output. Over the one-hour frequency that they are available, grid points within and just behind the leading edge of these bowing systems characteristically show sharp cooling through a deep layer in the lower to middle troposphere. It can be shown that this cooling is a direct result of feedbacks from the BMJ convective parameterization. For example, Fig. 8b shows the adjustment profiles computed by the BMJ scheme during the very early stages of the simulated system at a point over northeastern South Dakota. The convectively adjusted temperature profile computed by the scheme[2] is considerably colder than the initial sounding between cloud base (~ 850 hPa) and 550 hPa, then warmer between the mid-troposphere and cloud top, leading to the convective heating profile shown in Fig. 8c.

The shape of this vertical heating profile is commonly associated with the "trailing stratiform" region of propagating convective systems (e.g., Houze 1989). This shape assumes dynamic importance because of the local mesoscale response that it induces - primarily a response of subsidence (and adiabatic warming) in the layer where external cooling is imposed and upward motion (cooling) where parameterized warming is introduced (e.g., see Haertel and Johnson 2000). Plots of various fields along vertical cross sections through the mature simulated system provide strong evidence that this force-response relationship is active. First, it can be seen that the parameterized convective heating profile (Fig. 9a) is qualitatively unchanged at this later stage (although not shown, very little grid-scale latent heating occurs with this system). Associated with this heating profile are mid-level convergence, lower-tropospheric subsidence, and upper tropospheric rising motion, all occurring within and just behind the vertical columns where convective feedbacks are active (Fig. 9b). Streamline patterns suggest that the lower-tropospheric subsidence region has evolved into a mesoscale downdraft that diverges sharply just above the surface, producing low-level convergence and upward motion ahead of the system (Fig. 9b). By displacing and lifting ambient air, this mesoscale downdraft outflow appears to provide an important destabilizing mechanism that may be sufficient to activate the BMJ scheme in some surrounding grid points. Activation would be favored in any direction where ambient inhibition is small and other factors are favorable for deep convection. In the present case, the simulated convective system propagates to the southeast, sharply to the right of the large scale steering currents, but in a direction where inhibition is low (at least in terms of the factors that inhibit convective activation in the BMJ scheme) and instability is high.

A second, related mechanism may be operative as well. While the local response to parameterized heating acts to restore the atmosphere to a quasi-balanced state, the heating/cooling effectively radiates away from its source via a spectrum of zero frequency gravity waves, or buoyancy bores (e.g., see Bretherton and Smolarkiewicz 1989; Mapes 1993, 1998; Lane and Reeder 2001; Liu and Moncrieff 2004). The spectrum is dominated by modes that ultimately spread the same distribution of heating/cooling into the surrounding environment. For the parameterized heating distribution shown in Fig. 9a, the n = 1, full tropospheric mode emerges as a dominant component. In idealized convective environments this mode propagates outward at about 20 m s^{-1} with upward motion in the lower half of the troposphere and subsidence aloft (Fig. 10). Like the outflow from a mesoscale downdraft, the wave front associated with this buoyancy bore produces lower to middle tropospheric cooling and moistening, locally reducing convective inhibition and increasing the likelihood that the BMJ scheme is activated as the wave passes.

When streamlines are plotted in a system-relative framework, the picture that emerges is more consistent with this second mechanism in that the streamline pattern suggests the presence of a bore-like feature below 600 hPa (Fig. 9c). Furthermore, the propagation speed of the simulated convective system is close to the theoretical value for the n = 1 mode, suggesting that the system may be propagating in a wave-CISK-like manner (Raymond 1983, 1987; Xu and Clark 1984; Cram et al. 1992), with a near resonance between the n = 1 buoyancy bore and the quasi-continuous reinforcement of this bore by newly activated convective grid points. While this evidence is intriguing, it is far from conclusive.

[2] Computation of convective adjustment profiles by the BMJ scheme is described briefly in section 5 and in detail in Baldwin et al. (2002).

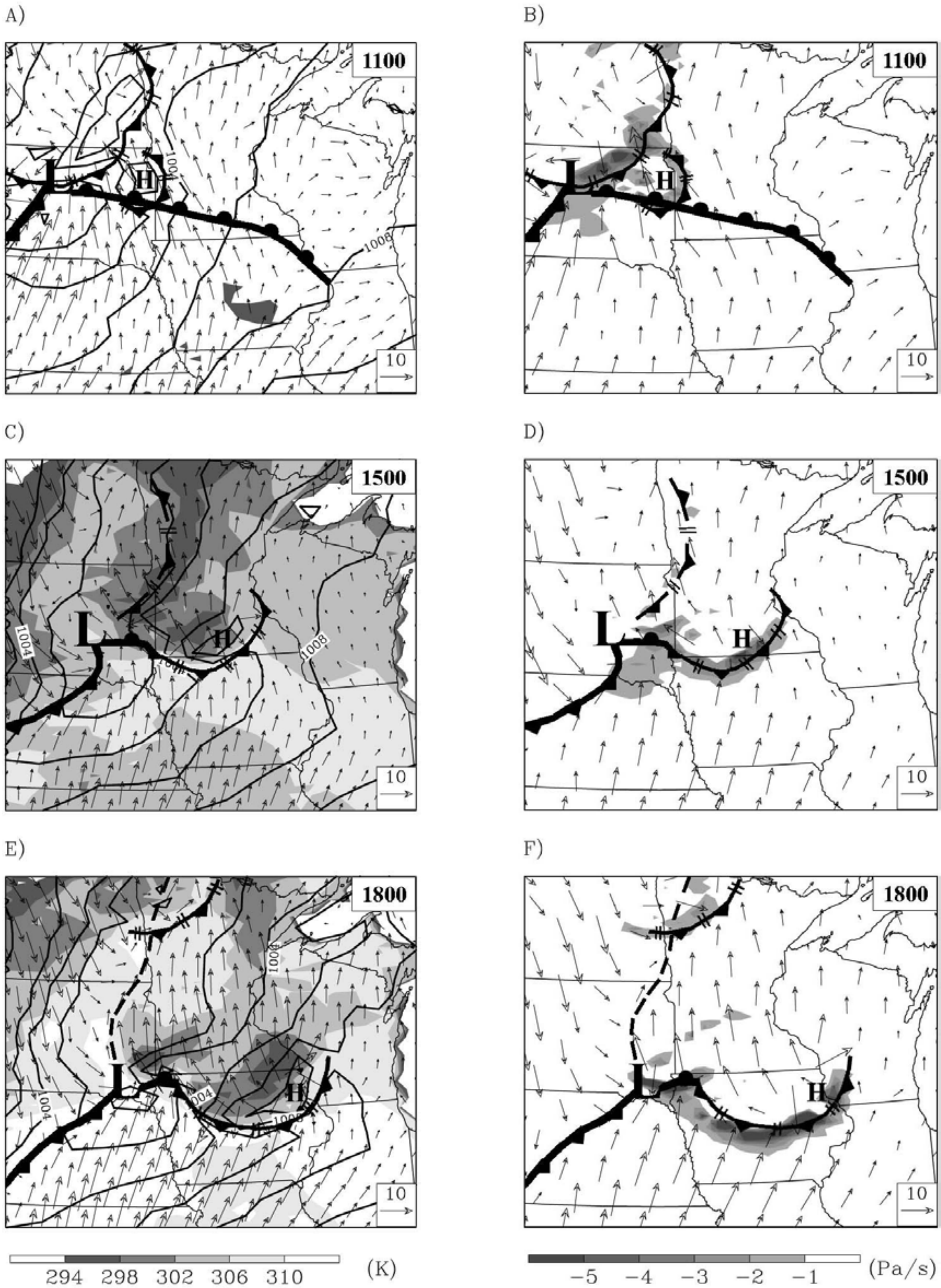

Fig. 6. Maturation of the bowing, propagating convective system in the control simulation. Left panels show sea-level pressure (2 hPa interval), 1000 hPa wind vectors, and surface-layer temperature (shaded, K); right panels show 700 hPa vertical pressure velocity (shaded, Pa s^{-1}), and low-level wind vectors. Times shown are 1100 UTC (a, b), 1500 UTC (c, d), and 1800 UTC (e, f). Mesoanalysis conventions follow Young and Fritsch (1989).

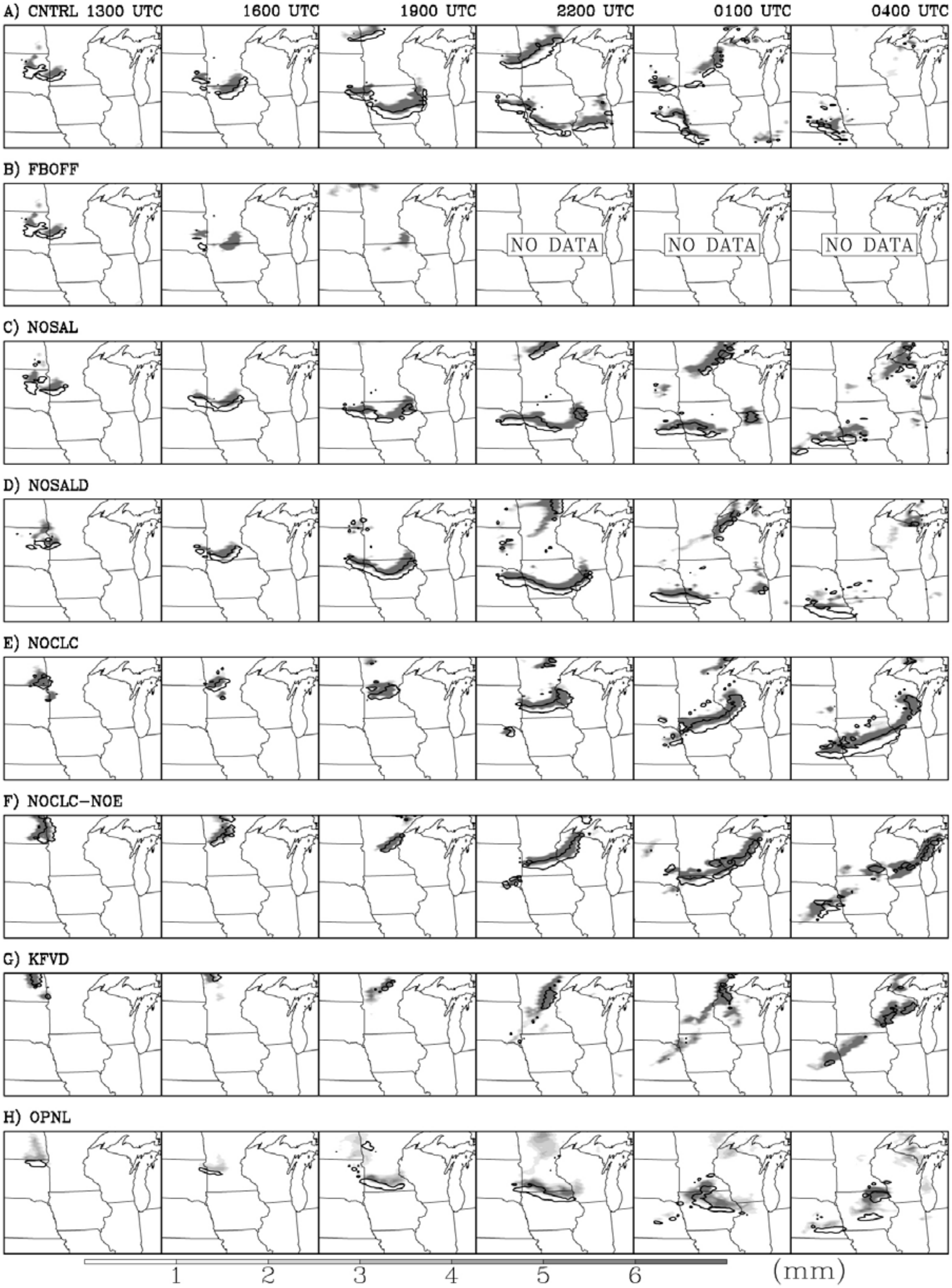

Fig. 7. 1h total surface precipitation accumulation (mm) and 700-hPa pressure vertical velocity (contours, 0 to -16 by 4 Pa/s) starting at 1300 UTC 11 June 2001 from runs: a) control; b) no convective feedback (4.a.); c) no lagged downdrafts, weakened cloud-layer cooling (4.b.1); d) as in c), but with artificial instantaneous cold pool (4.b.2) e) artificial instantaneous cold pool, no parameterized cloud-layer cooling (4.b.3); f) as in e), but without grid-scale evaporative cooling (4.b.4); g) KF heating algorithm used within BMJ scheme (4.c); and h) operational BMJ (4.d).

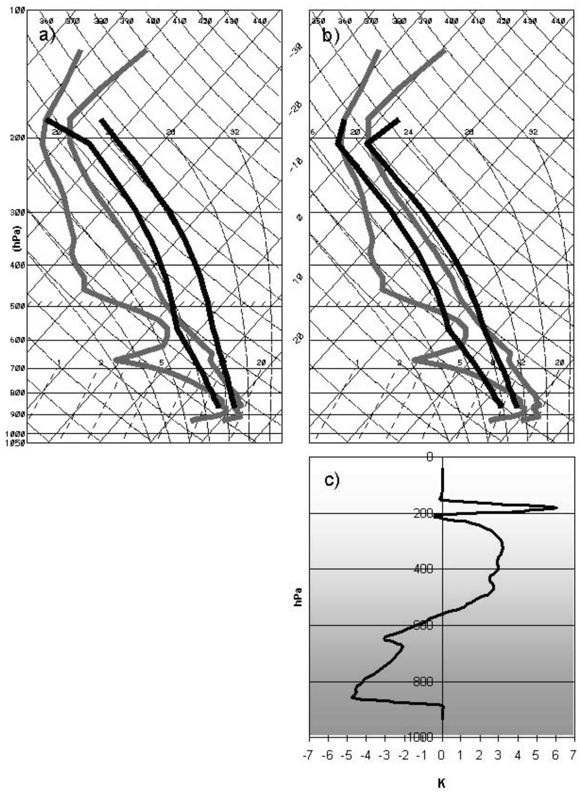

Fig. 8. Convective adjustment using the BMJ scheme for a point in northeast South Dakota around 1000 UTC in the control run. a) input environment temperature and dewpoint temperature (dark grey) with first-guess BMJ adjustment profiles overlaid (black). b) as in a), except final adjustment profiles (after imposing conservation of enthalpy) in black. c) vertical heating profile (K) corresponding to the final adjustment profiles in b).

If this diabatically driven system is propagating at the same speed and in resonance with a buoyancy bore, the circulations associated with the bore itself may be obscured by other circulations and processes

Finally, it is worth noting that a third factor likely plays some role in propagation of the simulated system. This factor is outflow from a low-level cold pool that develops through a separate mechanism related to parameterized convective feedbacks. This cold pool is evident in the surface temperature field (Figs. 6a, c, e) and temperature perturbation cross-sections (e.g., Fig. 9d). It is not created directly by the BMJ feedbacks (the scheme does not change the environment below cloud base), but it arises as a direct result of convective feedbacks. Specifically, in this environment the BMJ scheme cools so strongly near cloud base that the lapse rate between this level and the surface actually becomes super-adiabatic. This structure triggers the turbulence scheme, which effects a downward transport of the low-θ_e air created in the cloud layer by the BMJ scheme as it stabilizes the super-adiabatic layer. Since this two-step process takes time to evolve, the low-level downdraft lags behind the dominant parameterized convective tendencies.

While it seems possible that all three of these factors play active roles in promoting propagation of the simulated system, isolation and quantification of the individual roles has proven to be beyond the scope of this paper, so they are simply presented as potential contributors. What can be confirmed, however, is that the rather unusual heating profile generated by the BMJ scheme in this environment is the driving force for system propagation. In the next section, specific components of the BMJ heating profile are modified systematically in a series of tests designed to reveal the sensitivity of system propagation to different characteristics of the heating profile.

4. SENSITIVITY TESTS

For convenience, the following runs are summarized in Table 1.

4.1 Suppressing convective feedbacks within the mature system

The simplest way to demonstrate the importance of convective feedbacks is to deliberately withhold them and examine the impact on system evolution. This approach was taken by rerunning the simulation but setting convective temperature and moisture tendencies to zero after the 15 h time. Convective precipitation was still allowed to accumulate normally beyond this time so that system movement and configuration could be inferred, but subgrid-scale convection was no longer “felt” by resolved scales. Without the convective forcing, the precipitation system withered, its bow-shaped configuration morphed into a blob, and it lost its southerly propagation component, drifting off to the east with the mid-level flow (Fig. 7b). This test confirmed the importance of convective feedbacks to the configuration and propagation of the simulated system. The investigation then became one of determining what specific characteristics of the convective feedbacks were responsible for the propagation.

4.2 Systematically modifying the BMJ heating profile

The next step was to modify specific components of the BMJ heating profile. Each of these changes were introduced at t = 0 rather than the 15 h time. Within the BMJ scheme, these changes were introduced just prior to the feedback stage and did not affect moisture profiles or precipitation production. Consequently, enthalpy was no longer conserved in the scheme (see Janjic 1994 and Baldwin et al. 2002 for a discussion of the enthalpy conservation constraint), but interpretation of the results was simplified by limiting the modification to one variable.

4.2.1 Suppressing the lagged cold pool/weakening the cloud layer cooling

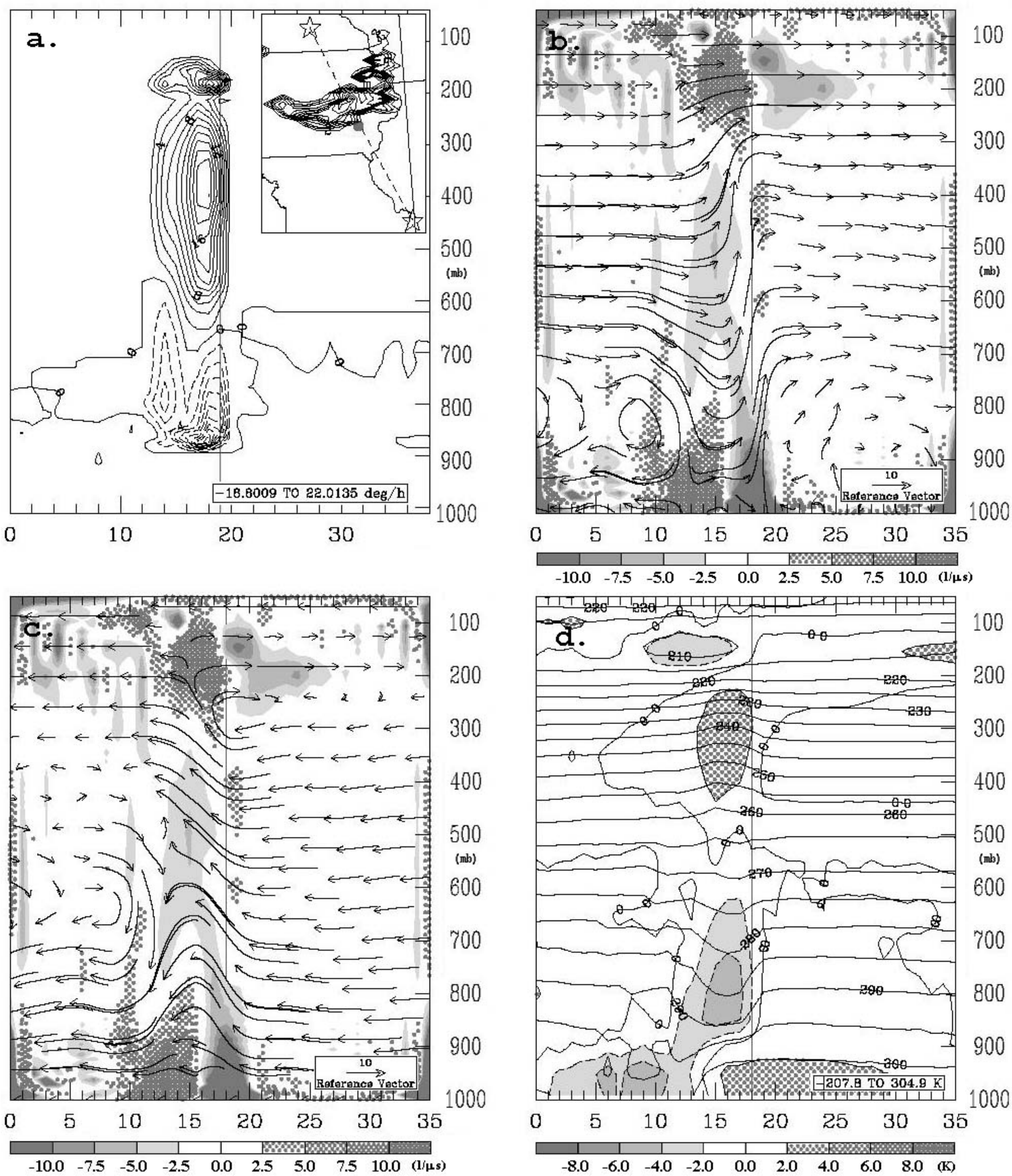

Fig. 9. Vertical cross sections through the mature convective system from the control run at 1900 UTC 11 June 2001. Horizontal axis for reference only. Distance between endpoints is about 433 km; each horizontal unit equals ~12 km. The vertical line at point 18 corresponds to the large centered dot on the cross section location image. a) Temperature tendency produced by the BMJ convective scheme (contour interval of 2 K h^{-1}) Inset: Cross section location through the 1 h precipitation field at 1900 UTC. b) Instantaneous flow (vectors; m/s) and divergence (shaded; s^{-1}) parallel to the cross section. c) System relative flow (vectors; m/s) and divergence (shaded; s^{-1}) parallel to the cross section (system velocity estimated at 18 m s^{-1}). d) Departure from level average temperature along the cross section (shaded; K) and temperature (contour interval 5 K).

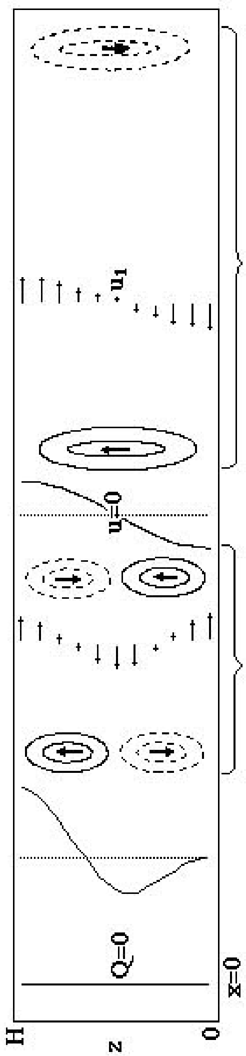

Fig. 10. (Fig. 6 from Mapes (1993)) Schematic of buoyancy bores, horizontal winds, and horizontal displacements of material lines after a given time for the heating profile used in Mapes (1993). The heating profile that initiated these bores is somewhat similar to those imposed in this study. A two mode heat source was forced near x = 0. Heating was then turned off after a given amount of time, yielding rolls in the opposite sense. ℓ = 1 corresponds to mode n = 0, and ℓ = 2 corresponds to mode n = 1 in this study.

The first modification was designed to assess the impact of the lagged cold pool on the propagating system. This cold pool was suppressed by altering the BMJ heating profile at all points where it would normally create a super-adiabatic structure. Specifically, the potential temperature at all levels in the BMJ reference temperature profile was constrained to be greater than or equal to the potential temperature (θ) in the surface layer. This modification effectively eliminated the lagged cold pool, though it also reduced the cloud layer cooling somewhat (e.g., see Fig. 11). When the simulation was run with this modification, system development was very similar to that seen in the control run. Specifically, a small area of convective activity developed in northeastern South Dakota, ahead of a larger area of eastward-moving convection just upstream, as in the control run. This leading activity rapidly expanded into a bowing line segment and propagated to the southeast, while the upstream system weakened and eventually disappeared. The propagating system appeared to be somewhat weaker and slower moving than with the unmodified BMJ scheme (cf. Figs. 7a and 7c), but its overall character was very similar.

4.2.2 Suppressing the lagged cold pool/weakening the cloud layer cooling/adding an instantaneous cold pool

The first test is revealing, but it leaves some uncertainty as to whether differences from the control run are due to suppression of the cold pool or weakening of the cloud-layer cooling. Although these two factors are not completely separable, one can place the emphasis on the latter effect by introducing a subcloud-layer cold pool through a separate mechanism. Thus, as a variation on the first test run, an instantaneous cooling tendency was introduced in the subcloud layer at all grid points where the superadiabatic layer was removed. This tendency was specified as part of the BMJ reference temperature profile (recall that the subcloud layer is not normally modified by the BMJ scheme). Specifically, the difference between the reference temperature and the ambient temperature in the surface layer was set equal to the difference between these two at cloud base (before removal of the superadiabatic layer). The magnitude of this subcloud cold anomaly was linearly reduced to zero between the surface and cloud base. This approach approximately restores the potential for cold-pool development, but retains the reduced cloud-layer cooling as in the first test. In this run, the bowing system appeared to be more cohesive and somewhat more progressive than in the run with no cold pool (cf. the 1900 and 2200 times in Figs. 7c and d), suggesting that the cold pool helps to focus and intensify low-level convergence on the leading edge of the system. At the same time, the system seems to develop and/or propagate more slowly than in the control run (cf. Figs. 7a and d), suggesting a sensitivity to the strength of the cloud-layer cooling.

4.2.3 Removing all cloud-layer cooling/adding an instantaneous cold pool

In the next test, cloud-layer cooling was removed altogether. As above, an instantaneous subcloud layer cold pool was introduced to provide some mechanism for low-level stabilization (in this case, numerical instability developed in the model when the subcloud cold pool was excluded). In this run (see Fig. 7e), precipitation features were quite similar to the original run through the 11h time, when the key convective activity developed over northeastern South Dakota. This feature developed as in the previous runs (see 1300 UTC in Fig. 7e), but instead of expanding, bowing, and beginning to propagate southward, it intensified briefly then slowly weakened as it drifted eastward into south-central Minnesota. Meanwhile, in contrast to the original run, the upstream system maintained its character and intensity. Eventually it absorbed the weakening system that had dominated in the previous runs. The combined system began to intensify, expand, and propagate in central Minnesota around the 18h time. Subsequently, this second system rapidly developed into an intense bowing, southwardly propagating system (Fig. 7e). The configuration, location, and timing of the quasi-linear portion of this system bear a striking resemblance to the observed system, including a "comma-head" structure on the northeastern end. Although there is no evidence of a broad area of "stratiform" precipitation that was observed to the west and north of the observed system, detailed analysis does reveal active grid-resolved microphysical processes, particularly near and just to the west of the comma head. Very little resolved precipitation reaches the ground, but condensational warming and evaporative cooling tendencies aloft (not shown) are comparable to parameterized convective heating and cooling rates.

4.2.4 Removing all cloud-layer cooling/adding an instantaneous cold pool/removing grid-scale evaporative cooling

The last two tests provide compelling evidence that parameterized *cloud layer* cooling plays a critically important role in the expansion of an isolated area of convection over northeastern South Dakota into a bowing, southward propagating mesoscale system. The low-level cold pool appears to play a secondary role, at least in the formative stages of this particular system. The cold pool may be relatively unimportant in the early stages because a stable nocturnal boundary layer prevails. Later in the day, however, the parameterized convective cold pool is embedded within a warmer environment, creating a stronger local anomaly that may promote the strong propagation seen after 1900 UTC in the previous sensitivity test. At the same time, however, detailed analysis reveals that a strong heating/cooling dipole (not shown) develops as a result of grid-resolved precipitation processes in this run with no parameterized cloud-layer cooling. Thus, it is possible that system propagation in this test after 1800 UTC is enhanced by an elevated resolved evaporative cooling anomaly that has a dynamic effect similar to the parameterized cloud-layer cooling.

The potential impact of grid-resolved evaporative cooling on this later-developing system was investigated by simply "turning off" evaporative cooling effects in the model. When this change was imposed, system development was similar to that in the previous run (with normal evaporative cooling) through about 2200 UTC, except that the isolated convective activity in northeastern South Dakota never developed. Nonetheless, between 1900 and 2200 UTC, a quasi-linear system took shape and expanded over south-central Minnesota in both runs (cf. Figs. 7e and f). With no evaporative cooling, however, the system was relatively ill-defined, never developing a comma-head configuration or strongly bowing presentation (cf. the 0100 and 0400 times in Figs. 7e and f). This result suggests that an elevated cold pocket created by grid-resolved evaporative cooling may help to organize and promote propagation of the mesoscale system much like the parameterized cloud-layer convective cooling. Alternatively, one could argue that the heating profile imposed by the unmodified BMJ scheme in this environment may help to focus upscale growth and mesoscale convective organization in much the same way that latent heating/cooling effects do in explicitly resolved simulations of convective systems (e.g., see Pandya and Durran 1996).

ID	Run Description	Section
CNTRL	Control BMJ run	3
FBOFF	No convective feedbacks (run until 21 h)	4.a
NOSAL	Suppressed lagged downdraft and weakened cloud-layer cooling	4.b.1
NOSALD	As in NOSAL, but with added artificial instantaneous cold pool	4.b.2
NOCLC	No parameterized cloud-layer cooling, added instant cold pool	4.b.3
NOCLC-NOE	As in NOCLC, but with grid-scale evaporative cooling turned off	4.b.4
KFVD	KF vertical distribution algorithm within the BMJ scheme	4.c
OPNL	Run using operational BMJ code	4.d

Table 1. Name, description, and discussion location of model runs used in this study.

4.3 Using another convective parameterization to generate the convective heating profile

This event was also simulated using the Kain-Fritsch convective parameterization (Kain 2004 –

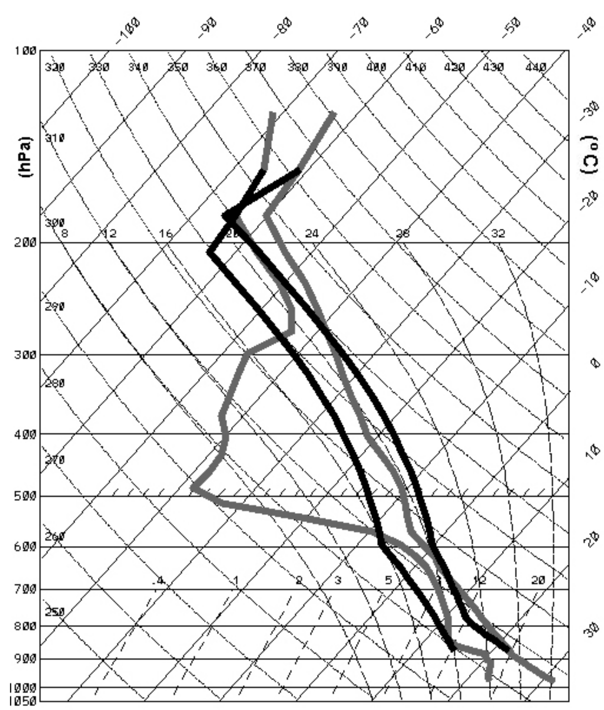

Fig. 11. Convective adjustment using the BMJ scheme modified as described in section 4.b.1 for a point in southeastern Iowa. Input sounding and final BMJ reference profiles are plotted as in Fig. 8. Note that the lower portion of the reference temperature profile is set equal to the potential temperature of the surface layer.

hereafter KF) in place of the BMJ scheme. This simulation (not shown) produced a swath of heavy precipitation in association with larger-scale forcing from eastern Wisconsin eastward across the Great Lakes region, but nothing resembling a bowing MCS. However, it was not clear whether the very dissimilar solution and the absence of a propagating convective system was due to a different parameterized heating profile, trigger function, or some other characteristic of the KF scheme.

In order to focus on the impact of the heating profile, the KF scheme's algorithm for vertically distributing the effects of convection was inserted into the BMJ code. In particular, the normal BMJ code was used to determine whether deep convection should be activated and, if so, how much vertically integrated latent heating (directly proportional to the precipitation rate) should occur. The KF cloud model was used to distribute the latent heating and convective drying in the vertical, without changing the vertically integrated magnitudes. This hybrid convective scheme typically produces heating profiles that are quite different from those generated by the BMJ scheme. For example, when the scheme is fed the input sounding shown in Figs 8a and b, it returns positive temperature tendencies at all levels throughout the cloud layer, with the exception of a shallow overshoot layer above 200 hPa (Fig. 12). Although there is some weak cooling in the subcloud layer, there is a notable absence of cooling in the lower to middle troposphere. In this case, an even more dramatic difference can be seen in the peak values of heating and cooling (compare the scales in Figs. 8c and 12). Peak values from the BMJ scheme are about an order of magnitude larger than those from the KF cloud model, even though the net column heating (net condensation and production of precipitation) is identical.

When the hybrid scheme is used to simulate the 11 June 2001 event, the result is quite similar to that obtained with the full KF scheme. Convection develops north of the surface low and eventually builds down along the cold front, but a cohesive propagating system never forms (Fig. 7g). Given the difference in peak heating/cooling magnitudes, it is not hard to see why the BMJ vertical distribution scheme induces a stronger dynamic response.

It is worth noting that a second hybrid scheme was created by matching parts of the two schemes in the opposite way – the BMJ vertical distribution algorithm was inserted in the KF scheme. When this code was used in the simulation, multiple bowing mesoscale systems formed in a solution that was less realistic than the BMJ run (not shown). The hybrid simulations provide further evidence that upscale growth and the development of bowing, propagating mesoscale systems is closely linked to the distinctive heating profile produced by the BMJ scheme in this environment.

4.4 Running the operational version of the BMJ (1/6 tendencies)

As mentioned in section 3a, the control run and all sensitivity tests discussed above used amplified convective feedbacks. Specifically, the feedback rate was six times the value used in the operational version of the BMJ. When this simulation is run with the (ca. 2001) operational BMJ code, a bowing, propagating MCS does develop, but it is relatively slow to emerge as a distinct feature, propagates more slowly, and is weaker. For example, at 1800 UTC the bowing system is just taking shape over south-central Minnesota (Figs. 13a and b; compare to Figs. 5e and f) and by 2100 UTC it has expanded and propagated southeastward into northeastern Iowa and southern Wisconsin (Figs. 13c and d). Although the system is clearly discernible as a propagating mesoscale feature, its presentation is not as impressive as the system produced with amplified convective feedbacks (cf. Figs. 7a and h). As suggested in section 3a, the run with magnified convective feedbacks was used as the control simulation for this study because it revealed a more clearly measurable linkage between convective forcing and the dynamic response, but the general character of the response appears to be the same at both levels of forcing.

5. DISCUSSION

Given the clear association between the BMJ heating profile and the formation of a bowing, propagating convective system in this case, one may wonder why such systems are not seen more frequently in model simulations using the BMJ scheme. An explanation requires some understanding of the

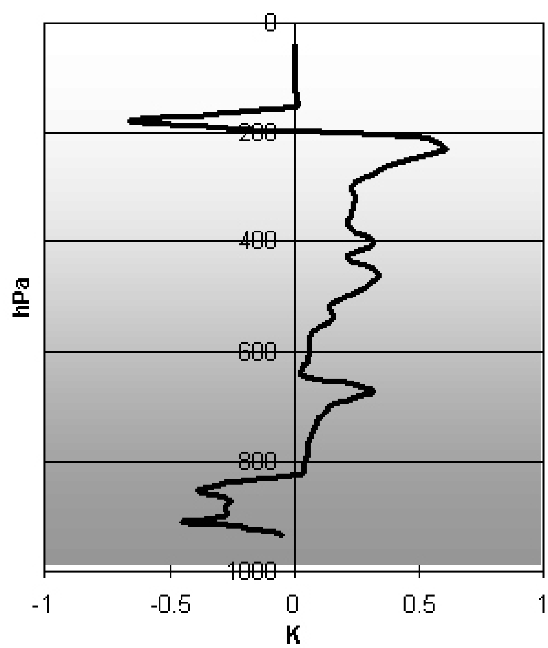

Fig. 12. Convective heating profile for the sounding shown in Fig. 8 using the BMJ scheme, but with the KF algorithm for vertical distribution of convective effects. Note that the absence of cloud-layer cooling in the lower to middle troposphere

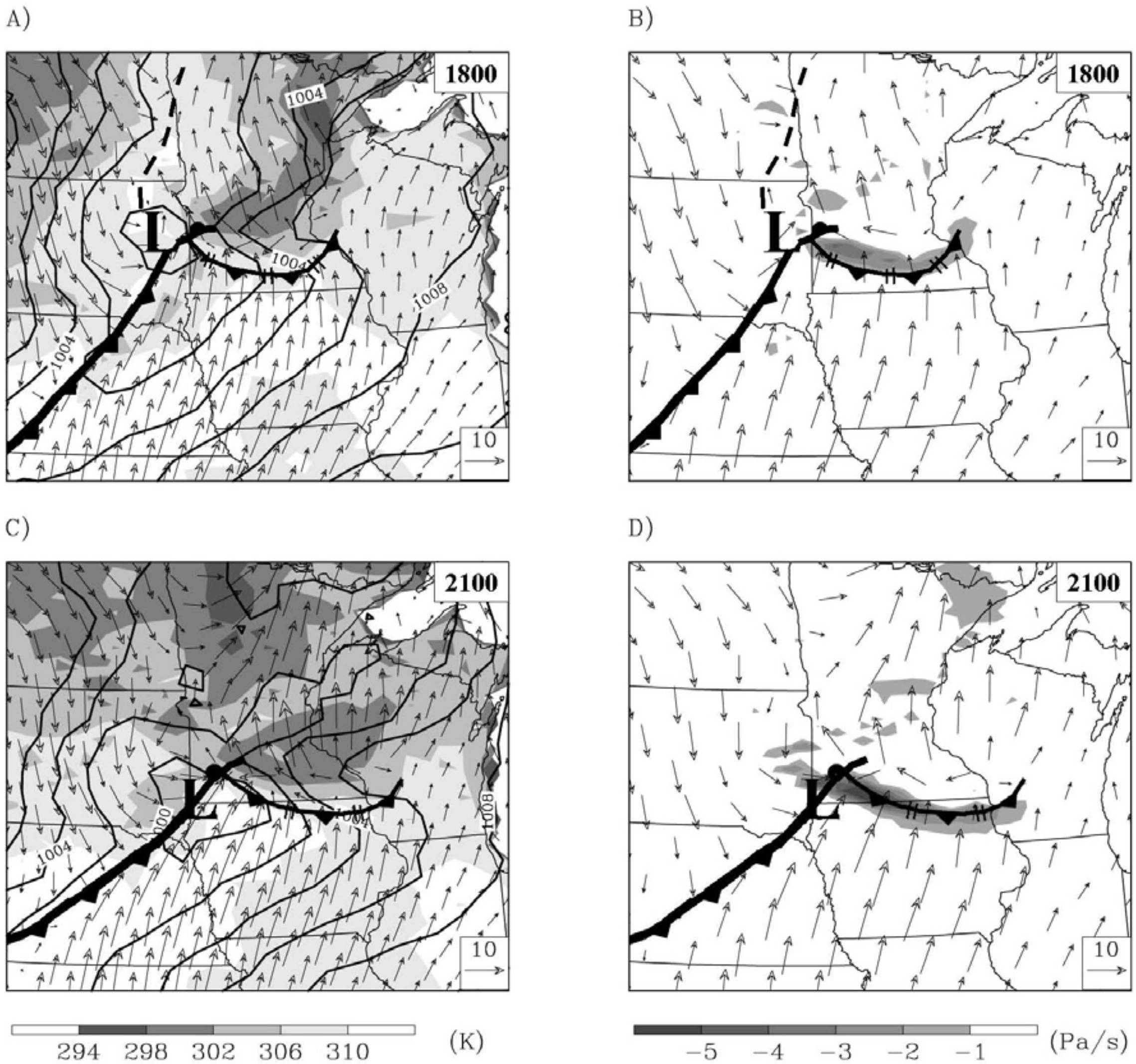

Fig. 13. As in Fig. 6, but for the run using the operational BMJ adjustment rates. Times shown are 1800 UTC (a, b), and 2100 UTC (c, d).

algorithm used by the BMJ scheme. For deep convection adjustment, the BMJ approach always nudges the ambient temperature profile towards a marginally unstable structure, i.e., a lapse rate that is slightly greater than the moist-adiabatic rate up to the freezing level, slightly less above. This is the characteristic "reference" temperature profile for the BMJ scheme (e.g., see Baldwin et al. 2002). When a profile like this is imposed upon a sounding containing a deep layer of much steeper lapse rates, large adjustments may be necessary in at least some layers. For example, Fig. 8a shows the "first-guess" BMJ reference profile overlaid on a simulated sounding from northeastern SD. Note that this first-guess profile is anchored to the sounding at cloud base, as specified in the BMJ algorithm (the scheme does not modify the sub-cloud layer). Because this anchor point has a high θ_e value, adjustment to the reference profile would require strong heating over a deep layer, particularly above the high-lapse rate layer extending up to ~ 500 hPa (Fig. 8c). However, as described in Baldwin et al. (2002), the BMJ scheme limits the magnitude of the net (vertically integrated) heating through a separate estimate of the amount of condensational warming that is possible in the column. When the estimated available condensational warming is less than what the first-guess reference temperature profile would provide, reconciliation of the two essentially amounts to shifting the reference temperature profile to the left on a skew-T/log P diagram. Given the parameter settings in the operational BMJ scheme, this process of enthalpy conservation produces the final reference profile and heating profile shown in Figs. 8b and c. As previously discussed, this profile is characterized by a heating/cooling dipole, with the transition occurring in the middle troposphere.

Note that the dipole is produced because the high lapse rate layer in the input sounding is essentially bisected by the near-moist-adiabatic reference temperature profile. The precise level where the two profiles cross depends on other factors, such as the deep-layer relative humidity, but in a qualitative sense, the deep-convective component of the scheme typically nudges a high-lapse-rate layer towards a moist adiabat by warming the top part of the layer (and above) while cooling the bottom part (and below). Furthermore, it is important to note that deeper layers of cooling are generated when high-lapse-rate layers are elevated well above cloud base. For example, in the sounding discussed above, the highest lapse rates are in the 550-650 hPa layer; the BMJ scheme warms above about 580 hPa, but cools from this level down to cloud base, at about 870 hPa. So, the scheme favors significant negative temperature feedbacks when high lapse rate layers exist and deep layers of cooling are favored when the most unstable layers are well above cloud base.

The presence of such temperature profiles is not uncommon over the Great Plains of the U.S., especially during the springtime (Carlson et al. 1983; Lanicci and Warner 1991), but it is likely that additional factors are required before bowing, propagating convective systems can be induced by the BMJ scheme. First, there must be sufficient cloud layer moisture to activate the scheme, or else no adjustment occurs. The steep lapse rates that can lead to parameterized heating/cooling dipoles tend to be associated with dry layers, which inhibit activation of the BMJ scheme. Next, the surrounding environment must be capable of supporting the operative upscale growth mechanisms. For example, local moisture and instability parameters should be just below the threshold values that would activate the BMJ scheme. With this backdrop, the modest lower-tropospheric lift induced at the leading edge of an incipient system could be sufficient to activate the scheme and reinforce the propagation mechanisms. Other characteristics of the surrounding environment are likely to play an important role as well. For example, these systems seem to form preferentially in environments with low cloud-layer wind shear; if gravity-wave mechanisms are important, then stability parameters, especially those favoring wave ducting, could be important. All of these factors, and perhaps others, are likely to play some role in the formation and perpetuation of these bowing, propagating systems. Thus, these systems become a common feature in model forecasts only under certain meteorological regimes.

6. SUMMARY AND CONCLUSIONS

Bowing, propagating precipitation systems are occasionally seen as prominent features in output from the Eta model and other models that use the BMJ convective parameterization, especially during the spring and early summer. Although these features have attracted attention for years (especially among forecasters), an explanation for their origin, mechanism of upscale growth, and meteorological significance has never been offered. Such an explanation is provided in this study, based on diagnostic analysis of a simulated bowing, propagating system that appeared in Eta model output on the same day that a damaging MCS moved through the western Great Lakes region in June of 2001.

Based on this study, it appears that these systems form as a dynamic response to an unusual convective heating profile imposed by the BMJ convective scheme in certain environments. This profile is characterized by a heating/cooling dipole, with heating in the upper half of the parameterized cloud layer and cooling in the lower half. The precise nature of the upscale growth mechanisms associated with this heating profile is not identified in this study, but three likely components of the upscale growth are identified. The first is a mesoscale downdraft induced by deep lower-to-middle tropospheric cooling. Outflow from this downdraft appears to organize and focus convergence along the leading edge of the propagating system. The second is a convectively induced buoyancy bore. This feature produces lower-tropospheric upward motion as it propagates into the adjacent environment. The third component is a boundary-layer cold pool that is produced indirectly by the convective scheme in this environment. As with the outflow from the mesoscale downdraft, this cold pool seems to focus and enhance lower-tropospheric upward motion along the leading edge of the system. Each of these mechanisms destabilizes the adjacent atmosphere and decreases convective inhibition in nearby grid columns, promoting new convective development, expansion, and propagation of the larger system. Propagation tends to favor the path of least resistance in the environment, which could be the direction where inhibition is lowest or perhaps the direction where low-level inflow is maximized (e.g., see Corfidi 2003).

The integral role of the heating profile and, in particular, its lower-to-middle tropospheric cooling component, was confirmed in this study through a series of sensitivity tests. These tests showed that the configuration and propagation characteristics of the focal convective system were very sensitive to the strength of the cloud-layer cooling imposed by the BMJ scheme. When this cooling was reduced, the emergence of the propagating system was delayed and the system was weaker. When cooling was completely eliminated, initial convective activity failed to evolve into a bowing, propagating system. Interestingly, a propagating system eventually developed under these conditions, but in a different location and under the influence of a grid-resolved heating/cooling dipole similar to the parameterized feature. System characteristics were also sensitive to the strength of a low-level cold pool that lagged behind the leading edge of the propagating system. When formation of this cold pool was suppressed, the propagating system was somewhat less intense and slower moving.

The question posed in the title of this paper is: Are the propagating bow-shaped features frequently seen in Eta-model output “for real”? They seem to be realistic, in the sense that they represent a dynamically consistent response to diabatic forcing. Yet, our experiences in working with forecasters at the SPC suggest that, more often than not, the predicted systems have no observational counterpart. Although they are often predicted by the model in meteorological regimes that are supportive of possible bow echoes, their emergence is not limited to these situations. Furthermore, even when they are associated with appropriate regimes, they rarely show correspondence with observed systems on time and space scales that are useful for regional weather prediction. Thus, while their association with observed systems is intriguing, the false alarm rate for their prediction by the Eta model is too high to make them reliable predictors of real bow echoes.

Acknowledgements

SPC forecasters, especially Steve Wiess and Paul Janish, are thanked for providing some of the initial motivation for this study, as well as many useful discussions and suggestions. Thanks also to Dave Stenstrud, Kelvin Droegemeier, and Lance Leslie for providing guidance throughout the course of this work, to Lou Wicker for assistance with NCL and insightful discussion, and to Brett Morrow and Steve Fletcher for technical support. This work was funded by NOAA OAR EEO and by a grant to OU CAPS from Williams Energy Marketing and Trading, Inc.

REFERENCES

Baldwin, M. E., J. S. Kain, M. P. Kay, 2002: Properties of the convective scheme in NCEP's Eta model that affect forecast sounding interpretation. *Wea. Forecasting*, **47**, 1063-1079.

Betts, A.K., 1986: A new convective adjustment scheme. Part I: Observational and theoretical basis. *Quart. J. Roy. Meteor. Soc.*, **112**, 677-691.

Black, T. L., 1994: The new NMC Eta model: Description and forecast examples. *Wea. Forecasting,* **9**, 265-278.

Bretherton, C. S., and P. K. Smolarkiewicz, 1989: Gravity waves, compensating subsidence and detrainment around cumulus clouds. *J. Atmos. Sci.*, **46,** 740–759.

Carlson, T. N., S.G. Benjamin, G.S. Forbes and Y.-F. Li, 1983: Elevated mixed layers in the regional severe storm environment: Conceptual model and case studies. *Mon. Wea. Rev.,* **111**, 1453–1474.

Corfidi, S. F., 2003: Cold pools and MCS propagation: Forecasting the motion of downwind-developing MCSs. *Wea. Forecasting*, **18**, 997–1017.

Cram, J.M., R.A. Pielke, and W.R. Cotton, 1992: Numerical simulations and analysis of a prefrontal squall line. Part II: Propagation of the squall line as an internal gravity wave. *J. Atmos. Sci.*, **49**, 209-225.

Fujita, T., 1955: Results of detailed synoptic studies of squall lines. *Tellus*, **4**, 405-436.

Haertel, P. T., and R. H. Johnson, 2000: The linear dynamics of squall line mesohighs and wake lows. *J. Atmos. Sci.*, **57**, 93-107.

Houze, R. A., 1989: Observed structure of mesoscale convective systems and implications for large-scale heating, *Quart. J. Roy. Meteor. Soc.*, **115**, 425-461.

Janjić, Z.I., 1994: The step-mountain Eta coordinate model: Further developments of the convection, viscous sublayer, and turbulence closure schemes. *Mon. Wea. Rev.*, **122**, 927-945.

_____, 2003: A nonhydrostatic model based on a new approach. *Meteorol. Atmos. Phys.*, **82**, 271-285.

Kain, J. S., M. E. Baldwin, P. R. Janish, S. J. Weiss, M. P. Kay and G. W. Carbin, 2003: Subjective verification of numerical models as a component of a broader interaction between research and operations**.** *Wea.Forecasting*, **18**, 847–860.

____, 2004: The Kain-Fritsch convective parameterization: An update. *J. Appl. Meteor.*, **43**, 170-181.

____, S. J. Weiss, J. J. Levit, M. E. Baldwin, and D. R. Bright, 2005: Examination of near-convection-resolving configurations of the WRF model for the prediction of severe convective weather: The SPC/NSSL Spring Program 2004. Submitted to *Wea. Forecasting*.

Lane, T. P., and M. J. Reeder, 2001: Convectively generated gravity waves and their effect on the cloud environment. *J. Atmos. Sci.,* **58**, 2427–2440.

Lanicci, J. M., and T. T. Warner, 1991: A synoptic climatology of the elevated mixed-layer inversion over the southern great plains in spring. Part I: Structure, dynamics, and seasonal evolution. *Wea. Forecasting*, **6**, 198–213

Liu, C., and M. W. Moncrieff, 2004: Effects of convectively generated gravity waves and rotation on the organization of convection. *J. Atmos. Sci.*, **61**, 2218-2227.

Mapes, B. E., 1993: Gregarious tropical convection. *J. Atmos. Sci.*, **50**, 2026-2037.

____, 1998: The large-scale part of tropical mesoscale convective system circulations: A linear vertical spectral band model. *J. Meteor. Soc. Japan*, **76**, 29-55.

Pandya, R. E., and D. R. Durran, 1996: The influence of convectively generated thermal forcing on the mesoscale circulation around squall lines. *J. Atmos. Sci.*, **53**, 2924–2951.

Przybylinski, R. W., 1995: The bow echo: Observations, numerical simulations, and severe weather detection methods. *Wea. Forecating*, **10**, 203-218.

Raymond, D. J., 1983: Wave-CISK in mass flux form. *J. Atmos. Sci.*, **40**, 2561-2572.

____, 1987: A forced gravity wave model of self-organizing convection. *J. Atmos. Sci.*, **44**, 3528-3543.

Weisman, M. L., 2001: Bow echoes: A tribute to T. T. Fujita. *Bull. Amer. Meteor. Soc.,* **82**, 97–116.

Young, G. S., and J.M. Fritsch, 1989: A proposal for general conventions in analyses of mesoscale boundaries. *Bull. Amer. Meteor. Soc.,* **70**, 1412–1421.

Zhao, Q., T. L. Black, and M. E. Baldwin, 1997: Implementation of the cloud prediction scheme in the Eta model at NCEP. *Wea. Forecasting*,**12**, 697–712.

Xu, Q., and J. H. E. Clark, 1984: Wave CISK and mesoscale convective systems. *J. Atmos. Sci.*, **41**, 2089-2107.